EPITAXIAL GROWTH

Epitaxy is a process whereby an oriented crystalline material, usually called the epitaxial layer, is deposited as an extension onto an existing oriented crystal, usually referred to as the substrate. Epitaxial growth can be further divided into two categories: homoepitaxy and heteroepitaxy. Homoepitaxy is the growth of a layer essentially identical to its substrate as in GaAs on GaAs. In heteroepitaxy, the epitaxial layer differs chemically from its parent substrate, as in $Al_xGa_{1-x}As$ on GaAs, provided both crystals have the same lattice constant. Lattice mismatched heteroepitaxy is also possible in the case where the epitaxial layer is very thin so that defects will not be generated.

Since the early 1960s, there has been strong interest in growing single crystalline multilayer compound semiconductor structures called heterostructures for device applications. Various deposition techniques such as liquid phase epitaxy (LPE) (1), vapor phase epitaxy (VPE) (2), and molecular beam epitaxy (MBE) (3) have been developed to fulfill the needs of ever complicated device structures. The process of LPE involves the precipitation of materials from a supersaturated solution onto an underlying substrate under near equilibrium conditions. The VPE process involves near-equilibrium gas phase chemical reactions of gaseous sources followed by surface reactions before incorporation into the epitaxial layer. However, in an alternative VPE process using metalorganic sources, called metal-organic chemical vapor deposition (MOCVD) (4), reactions are far from thermodynamic equilibrium. The MBE technique is also a thermodynamically nonequilibrium process. It involves the reaction of thermal beams of constituent atoms or molecules from solid sources with a crystalline substrate under ultra-high vacuum conditions. MBE using gaseous sources has also been developed. The attributes of these major epitaxy techniques are compared in Table 1.

LIQUID PHASE EPITAXY

The liquid phase epitaxy technique was first demonstrated by Nelson in 1963 to fabricate GaAs tunnel diodes and homojunction lasers from molten metal solutions (5). Since then, LPE technology has been used successfully to fabricate various types of electronic and optical devices using compound semiconductor materials. Basically, LPE involves the growth of an epitaxial layer from a supersaturated solution on a single crystal substrate that has a similar crystal structure and lattice constant to the growing layer. The supersaturated solution is brought in contact with the substrate for a desired period of time. Depending on the degree of supersaturation in the solution and the contacting time between the solution and the substrate, the amount of material that precipitates onto the substrate can be controlled precisely.

The thermodynamic basis of LPE can be illustrated by the generalized binary (AB) phase diagram shown in Fig. 1, where A and B are the group III element and group V element, respectively. In general, the growth solution is rich in one of the major components of the epitaxial layer and dilute in all others. For III–V compound semiconductors, it is usually possible to use the group III metal (i.e., Ga and In) as the solvent for the group V elements such as As, P, and Sb. For example, based on the fact that the solubility of As (element B) in Ga-rich (element A) solutions decreases with decreasing temperature, one can use a Ga-rich solution saturated with As for LPE growth of GaAs. At temperature T_2, the Ga solution is saturated with x_2 atomic percent of As. Cooling the solution to T_1, where x_1 is the corresponding equilibrium atomic percentage of As in the solution, creates a driving force for the precipitation of a congruent compound AB (i.e., GaAs) until the new saturation condition is reached. At the proper

Table 1. Summary of the Characteristics of Epitaxial Methods Used for the Growth of III-V Compound Semiconductors

Technique	Strength	Weakness
LPE	Simple and low-cost apparatus	Morphology and uniformity problems
	Excellent material quality	Small scale
		Graded interface
		Difficult to grow Al–In compounds
Trichloride VPE	Simple apparatus	No Al alloys
	High-purity materials	Difficult to grow alloys
Hydride VPE	Large-scale production system	No Al alloys
		Complex reactor design
		Use of toxic gases
MOCVD	Highly flexible	Expensive growth system
	Abrupt interfaces	Expensive reactants
		Use of toxic sources
MBE	Simple process	Expensive growth system
	High uniform	
	Abrupt interfaces	
	In situ monitoring and control	

J. Webster (ed.), *Wiley Encyclopedia of Electrical and Electronics Engineering*. Copyright © 1999 John Wiley & Sons, Inc.

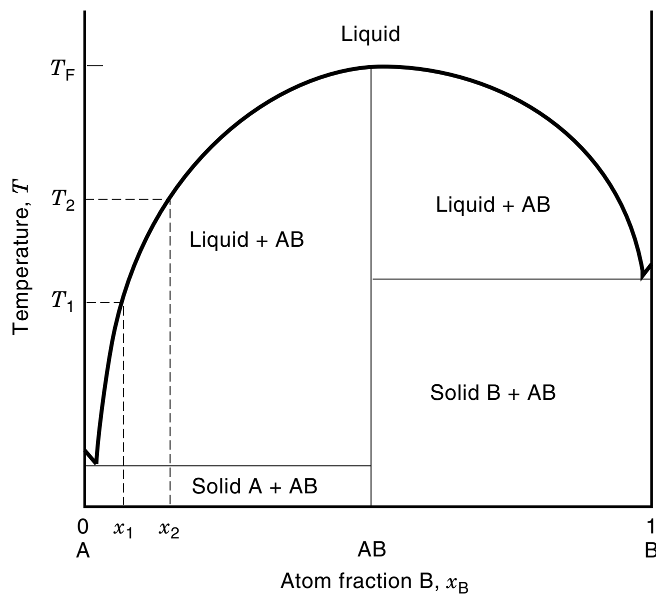

Figure 1. The temperature-composition phase diagram of the III–V binary compound $A^{III}B^{V}$. T_F is the congruent melting temperature of the component AB at which the solid and liquid have the same composition.

growth condition, some of the precipitates may be deposited as an epitaxial layer on a GaAs substrate that is in contact with this solution.

LPE Apparatus

The basic LPE process requires the use of experimental apparatus that permits growth solutions of desired compositions to be placed in contact with the substrate for periods under controlled temperature cycles. Three different growth techniques are used in LPE: the tipping technique in which solution-substrate contact is achieved by tipping the furnace; the dipping technique in which the substrate is dipped vertically into the solution; and the sliding technique in which the substrate is slid horizontally into contact with the solution. Tipping and dipping systems are comparatively simple and easy to operate. High-quality single epitaxial layers have been produced by both methods. However, such systems become inadequate for the growth of multilayer heterostructures required for many modern devices.

The sliding technique, which allows multilayer growth, has become the principle LPE method. Figure 2 illustrates a typical horizontal sliding LPE system. The main components of the apparatus are a graphite multibin-boat with a slider insert, a fused silica tube to provide a protective atmosphere, and a multiple zone resistance heating furnace. The graphite boat has a number of reservoirs, each of which contains a saturated solution corresponding to the epilayer to be grown. The desired electrical conductivity of epilayers can be controlled by adding impurities into the specific growth solutions. Typical n- and p-type dopants for LPE growth of III–V compounds are from column VI (Te and Se) and column II (Zn) of the periodic table, respectively. The group IV elements (Si, Ge, and Sn) are amphoteric dopants in III–V compounds. Its incorporation and the resultant electrical conductivity depend on the growth conditions. The substrate is placed in the recess of the graphite slider, which can be brought into contact with each solution in turn by sliding under different reservoirs. In this way, multilayer p–n junctions and heterostructures with desired compositions and thicknesses can be grown successfully on the substrate, and this operation can be automated easily. In order to ensure a clean wipe off of the melts and to prevent melt carryover between reservoirs, the clearance between the slider and the bottom of the reservoirs is optimized. The growth process is generally carried out under a hydrogen ambient to minimize oxidation of melts.

Phase Diagram

In order to control the alloy compositions and layer thicknesses precisely in LPE processes, it is necessary to determine appropriate phase diagrams that describe relationships between solids and liquids at different temperatures. Several authors have calculated phase diagrams for ternary (6) and

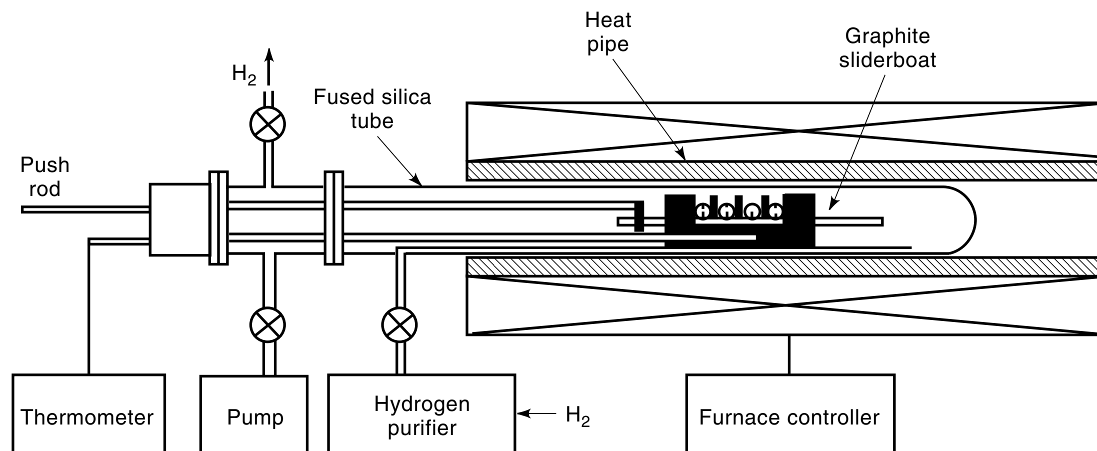

Figure 2. Schematic diagram of a sliding liquid-phase epitaxy system. The principal components of the LPE system are a graphite slider boat, a fused silica tube, and a resistance furnace. To ensure a uniform temperature over all growth melts, the graphite boat is situated inside a heat pipe thermal liner in the furnace.

quaternary compounds (7,8) using simple solution models and solubility data of binary compounds. In III–V alloys, the solution composition-temperature relationship of a binary compound such as GaAs can be described by a single solubility curve as shown in Fig. 1. When a ternary compound is formed by combining two binary compounds, a continuous solid solution with different compositions usually develops. This provides the freedom of selecting alloys with a specific lattice constant or bandgap energy. The composition of solutions that are in equilibrium with a solid phase is no longer a single-valued function of temperature as in binary compounds. The ternary liquidus relationships may be conveniently represented by a series of isotherms, each of which gives the concentrations of the two minor constituents in saturated solutions at a particular temperature. Such liquidus isotherms for the Ga-rich saturated solutions of the Al–Ga–As system between 700 °C and 1000 °C are shown in Fig. 3(a), where the atomic percentages of Al and As in the solutions are plotted against each other (6).

The ternary phase diagram also provides information about the relationships between liquid and solid phases at different temperatures. Taking advantage of the stoichiometric property of the III-V compounds, the solidus relationships are represented by isotherms giving the solid composition as a function of the concentration of one of the minor constituents of the solution. A set of such isotherms for the Al–Ga–As system between 700 °C and 1000 °C is shown in Fig. 3(b), where the mole fraction of AlAs in the epilayer (x in $Al_xGa_{1-x}As$) is plotted against the atomic fraction of Al in the saturated solution, x^l_{Al} (6). With the knowledge of the solidus relationships of the system, the epilayer compositions can be controlled precisely. For example, in the $Al_xGa_{1-x}As$ system, specifying x^l_{Al} and the temperature completely fixes the composition of the saturated solution through liquidus isotherms like those of Fig. 3(a).

In extending the thermodynamic treatment to $A^{III}_xB^{III}_{1-x}C^V_yD^V_{1-y}$ type quaternary compounds, such as $Ga_xIn_{1-x}As_yP_{1-y}$, the alloy may be considered as regular mixtures of four ternary compounds. Using quaternary alloys, an added degree of freedom for independent selection of lattice constant and bandgap energy may be obtained. For example, bandgap energies extending from 0.75 eV to 1.34 eV are readily adjustable in lattice-matched $Ga_xIn_{1-x}As_yP_{1-y}$ layers on InP. However, because of the uncertainties in various interaction parameters, the calculated equilibrium Ga–In–As–P phase diagrams are in poor agreement with experiments (8). Nevertheless, for the $Ga_xIn_{1-x}As_yP_{1-y}$ lattice matched on InP, the solidus and liquidus curves for different compositions at various temperature have been determined experimentally (9).

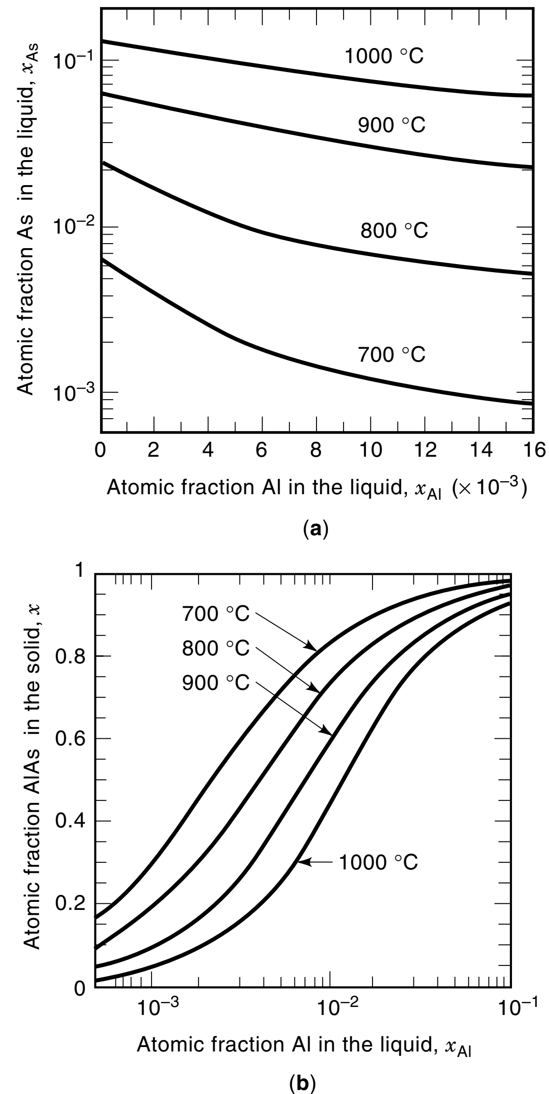

Figure 3. (a) Liquidus isotherms in the Al–Ga–As system between 700 °C and 1000 °C. The liquidus compositions of the saturated Al–Ga–As solution are related through the mass conservation relationship $x_{Al} + x_{Ga} + x_{As} = 1$. (b) Solidus isotherms for Al in $Al_xGa_{1-x}As$ alloys between 700 °C and 1000 °C. For example, to grow $Al_{0.6}Ga_{0.4}As$ from a saturated solution at 900 °C, the solidus isotherm indicates that a 0.01 atomic fraction of Al in the liquid (x_{Al}) is required. This Al liquidus composition fixes the saturation condition of the Al–Ga–As solution through the corresponding liquidus isotherms at 900 °C. The required As atomic fraction (x_{As}) to saturate the solution at 900 °C is 0.03. (Reprinted with permission from M. B. Panish and M. Ilegems, Phase equilibria in ternary III-V systems, *Progress in Solid State Chemistry,* Vol. 7, pp. 39–83, 1972. © 1972 Elsevier Science Ltd.)

LPE Growth Techniques

After growth parameters are determined through phase diagrams, epitaxial layers can be grown by LPE following the temperature cycle shown in Fig. 4. The furnace is initially heated above the saturation temperature T_0 and kept there for sufficient time to enable the melts to attain saturation. After equilibration, the temperature is ramped down at a linear rate, usually in the range 0.1 ~ 0.8 °C/min. Depending on the temperature where the substrate contacts the melt and the cooling procedure, there are four different LPE techniques. They are equilibrium-cooling, step-cooling, supercooling, and the two-phase method (10). All but the two-phase method provide a typical growth rate of ~1 μm/min. Because of the high growth rate, it is very difficult to grow thin layers (≤10 nm) by LPE.

The equilibrium-cooling technique employs a constant cooling rate throughout the growth cycle. The substrate is brought into contact with the solution at the saturation temperature T_0 to begin the growth. The growth is terminated by

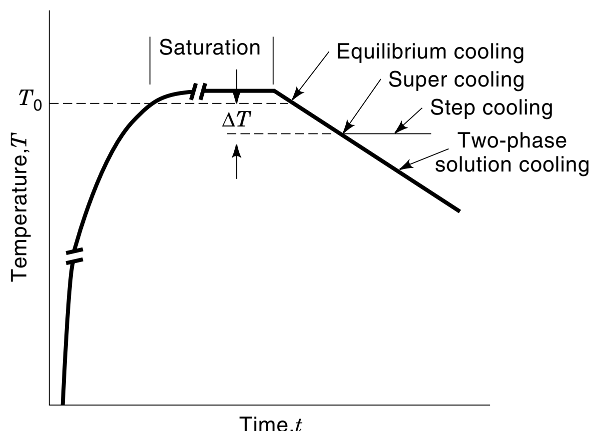

Figure 4. Temperature cycle and solution cooling procedure for liquid-phase epitaxy growth. T_0 is the equilibrium temperature of the saturated solution. The arrows indicate the times at which the growth solution is initially placed in contact with the substrate.

sliding the substrate with the epilayer out of the solution. The thickness of the grown layer d is determined by

$$d = \frac{2}{3} K \frac{dT}{dt} t^{3/2} \tag{1}$$

where t is the growth time and K is a constant that depends on the diffusivity of each solute and on the solute's mole fraction in the solution at the growth temperature.

In the step-cooling technique, the substrate and solution are cooled at a constant rate to a temperature ΔT below T_0 without spontaneous precipitation and then brought into contact. The constant temperature ($T_0 - \Delta T$) is maintained during the growth period. The thickness d of the grown layer is related to ΔT and the growth time t by the relation

$$d = K \Delta T t^{1/2} \tag{2}$$

The supercooling technique is a combination of equilibrium-cooling and step-cooling. The substrate is brought into contact with the solution when both are at a temperature ΔT below the saturation temperature of the solution. Cooling is continued without interruption at the same rate until growth is terminated. The thickness of the grown layer d is given by the sum of Eqs. (1) and (2), that is,

$$d = K \left(\Delta T t^{1/2} + \frac{2}{3} \frac{dT}{dt} t^{3/2} \right) \tag{3}$$

In the two-phase technique, the temperature is lowered far below T_0 for spontaneous precipitation to occur in the solution. Then the substrate and the solution are brought into contact, and cooling is continued at the same rate without interruption. This technique can be used to grow very thin layers because the presence of the precipitation reduces the growth rate.

VAPOR PHASE EPITAXY

Vapor phase epitaxy (VPE) refers to the formation of an epitaxial layer from a gaseous medium of different chemical composition. The VPE process involves vapor-phase transfer of the active species to the VPE reactor, followed by chemical reactions in the gas stream before being brought into contact with the substrate surface. When the appropriate molecule arrives at the surface, there must be adsorption and surface diffusion to a suitable growth site and desorption of the products not needed for growth. Unreacted gaseous reactants and products are thoroughly scrubbed and burned before being exhausted to the atmosphere.

In general, VPE is carried out in an open-tube flow system where transport results from forced convection induced by a rather large flow of a carrier gas. Hydrogen is often used as the carrier gas, and other inert gases such as nitrogen, argon, and helium have also been used. Commonly used reactants are either a gas or a volatile liquid at room temperature. In the latter case, the reactant is carried into the system by passing a carrier gas through the liquid. Reactant partial pressures and resident time in the deposition region are easily controlled externally by changing the gas flow rate using mass flow controllers. The reactor is heated by a multizone furnace (hot wall reactor) or a radio-frequency (RF) inductance heater (cold wall reactor) and can be operated either at atmospheric or low pressure. According to their gas flow characteristics, the VPE reactors can be classified in two categories: horizontal and vertical. In a horizontal reactor system, the flow of gases is parallel to the substrate surface. Because of the nature of the laminar flow of gases, a stagnant layer or boundary layer near the substrate surface is developed. The reactant species must diffuse in order to reach the substrate surface through this layer. Therefore, the growth rate varies as a function of the boundary layer thickness. In the vertical reactor design, the gas flow is perpendicular to the substrate surface. This geometry allows the incorporation of a rotating substrate holder design to improve the uniformity. However, thermal convection-induced turbulence alters the laminar flow conditions over the substrate.

Many chemical reactions have been employed for chemical transport of reactants in chemical vapor depositions. Among those useful for VPE growth of semiconductor materials are pyrolysis, reduction, synthesis, and disproportionation (11). For the VPE growth of III–V compounds, two methods are commonly used: (1) halide transport VPE and (2) metalorganic chemical vapor deposition. In the halide transport VPE system, chloride, bromide, and iodide transport agents have been used with success. However, further development was restricted to chloride VPE because only high-purity chloride species were readily available.

Chloride VPE

In chloride VPE of III–V binary compounds AB, the group III element (A) is transported in the form of metal chloride (ACl) and reacted with group V element (B) according to the reaction

$$4\mathrm{ACl} + \mathrm{B_4} + 2\mathrm{H_2} \rightarrow 4\mathrm{AB} + 4\mathrm{HCl} \tag{4}$$

Depending on the group III metal chloride generation method, chloride VPE is further classified into two categories: trichloride VPE and hydride VPE. Both epitaxy techniques are carried out in hot wall reactors composed of two zones set at different temperatures by using multizone furnaces.

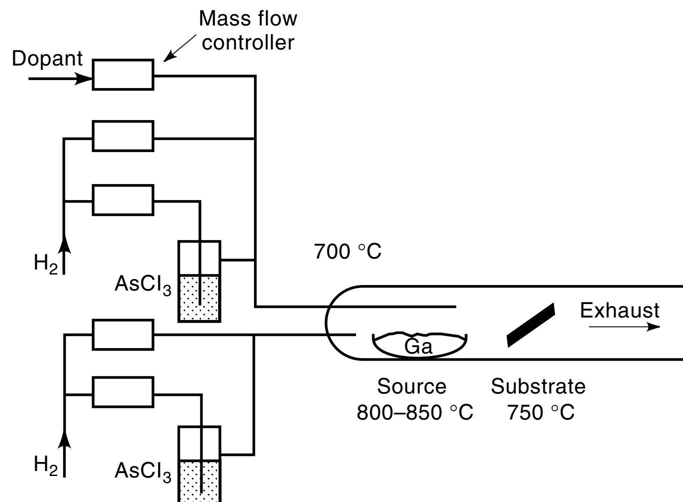

Figure 5. Schematic illustration of a trichloride vapor-phase epitaxy system for GaAs growth. HCl is first generated by decomposing $AsCl_3$ with H_2. The reaction of in situ generated HCl with the GaAs crust formed on the surface of the Ga source material provides the necessary GaCl and As_4 for deposition of GaAs at the low temperature deposition zone.

For the trichloride VPE process, the growth apparatus is shown in Fig. 5. In the process of growing GaAs, $AsCl_3$ is used as a source of As and as a reactant with GaAs to transport Ga by the formation of GaCl in the high-temperature source zone according to the following reactions:

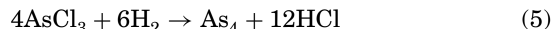

$$4AsCl_3 + 6H_2 \rightarrow As_4 + 12HCl \quad (5)$$

$$4Ga + As_4 \rightarrow 4GaAs \quad (6)$$

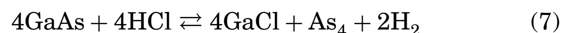

$$4GaAs + 4HCl \rightleftarrows 4GaCl + As_4 + 2H_2 \quad (7)$$

The $AsCl_3$ vapor is transported by a hydrogen carrier gas to the heated furnace and decomposed into As_4, HCl, and excess H_2. The As_4 dissolves in the liquid Ga source until the solution becomes saturated and a GaAs crust forms over the liquid surface as described by Eq. (6). By reaction of HCl with the GaAs crust in the high-temperature source zone, GaCl and As_4 are generated and transported to the low-temperature deposition zone for epilayer growth. These reactions are described by the same Eq. (7), and the reaction direction is determined by the temperature profile in the reactor. Because the equilibrium of the reaction in Eq. (7) is established only after the Ga has been saturated with As and a GaAs crust formed, it is vital to maintain a flat temperature profile over the source. A partial dissolution of the GaAs crust and the reaction of the exposed Ga with HCl lead to uncontrolled variations in the reactant concentrations that cause surface morphology problems and loss of growth rate control. This problem can be avoided by the use of a solid GaAs source. Single epilayer GaInAs and GaInAsP alloys have been prepared by this method.

One unique feature of trichloride VPE is the ability to achieve low background carrier concentration in epitaxial layers. This is due to the fact that $AsCl_3$ and PCl_3 can be distilled into very high purity liquids. This allows the fabrication of devices consisting of low doping layers. For the growth of intentionally doped layers, both trichloride and hydride VPE techniques use either gaseous or solid dopant sources to achieve the desired electrical conductivity. Doping with n- and p-type dopants are commonly accomplished with H_2S gas and Zn vapor, respectively.

For the hydride VPE process, the growth apparatus is very similar to that of the trichloride VPE and is shown in Fig. 6. In this process, GaCl is generated directly by passing HCl over the Ga source and As_4 from the pyrolysis of AsH_3 according to

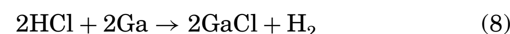

$$2HCl + 2Ga \rightarrow 2GaCl + H_2 \quad (8)$$

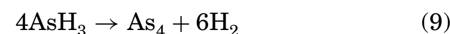

$$4AsH_3 \rightarrow As_4 + 6H_2 \quad (9)$$

These reactions supply GaCl and As_4 to establish the reaction of Eq. (4) or (7).

The generation of GaCl is accomplished by the complete reaction of HCl with Ga at temperatures above 800°C, and no critical temperature control over the source is required. In addition, the ability of independent generation of gas phase species allows variation of the Ga to As ratio. This is in contrast to the trichloride method where the Ga to As ratio is fixed by the reaction of Eq. (5). These properties make the hydride method a preferred growth technique among chloride VPE techniques. For example, it has been used for the mass production of $GaAs_{1-y}P_y$ epitaxial layers on GaAs and GaP substrates for light-emitting diode applications. Most of the VPE growth of GaInAsP alloys has also been done by the hydride method (12). Nevertheless, because of the many chemical reactions involved in the quaternary alloy growth, modeling is complex and difficult. Predicting alloy composition from vapor flows is further complicated by the formation of deposits on the reactor wall. Therefore, proper gas flows to achieve desired compositions must be determined empirically.

Because the chloride VPE reactions require some time to achieve equilibrium after altering the flow rates, it is not practical to grow multilayer structures by changing flow rates. One solution is to use a multichamber reactor design where gas reactants for each layer are supplied through separate reaction chambers. After the gas flow equilibrium has been established in each chamber, heterostructures can be

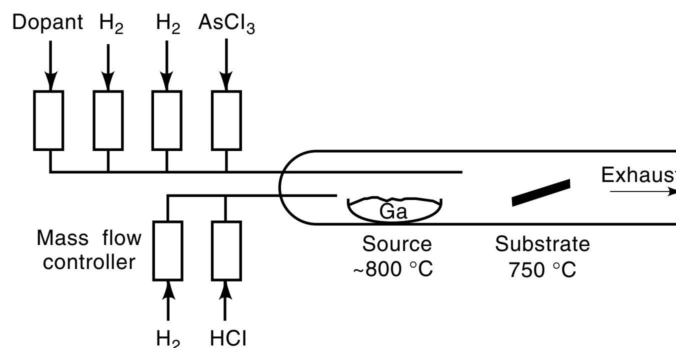

Figure 6. Schematic illustration of a hydride vapor-phase epitaxy system for GaAs growth. The growth sources, GaCl and As_4, are generated in different temperature zones. The pyrolysis of AsH_3 in the low temperature growth zone provides As_4. GaCl is generated by reaction of HCl with Ga in the high temperature source zone.

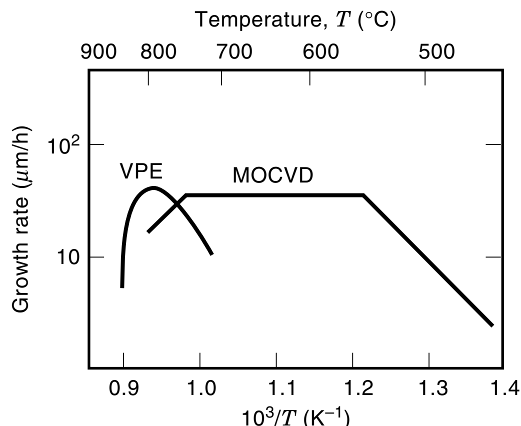

Figure 7. Temperature dependence of GaAs growth rate on (100) GaAs substrates for typical trichloride VPE and MOCVD.

grown by introducing the substrate into designated reaction chambers sequentially.

In trichloride and hydride VPE methods, the temperature-dependent growth rates are qualitatively similar and shown in Fig. 7 (13). At low temperatures, the growth rate is kinetically limited by the reduction of chemisorbed As–Ga–Cl complexes to form GaAs. This is evident from the substrate-orientation-dependent growth rates. In the low-temperature regime, the growth rate increases with the temperature. When the temperature is increased, the growth is mass-transfer-limited by the diffusion of reactants to the substrate and causes a decrease of growth rate, which is independent of the substrate orientation.

Metalorganic Chemical Vapor Deposition

The MOCVD technique was pioneered by H. M. Manasevit in 1969 to grow GaAs on various substrates using a metalorganic Ga source mixed with arsine (14). It is also referred to as organometallic VPE (OMVPE) or organometallic CVD (OMCVD). the MOCVD system is simpler than the chloride systems. The growth of GaAs by the pyrolysis of vapor phase mixture of AsH_3 and $Ga(CH_3)_3$ (trimethylgallium, TMG) or $Ga(C_2H_5)_3$ (triethylgallium, TEG) typifies the process. As shown in Fig. 8, TMG or TEG vapor is transported into the

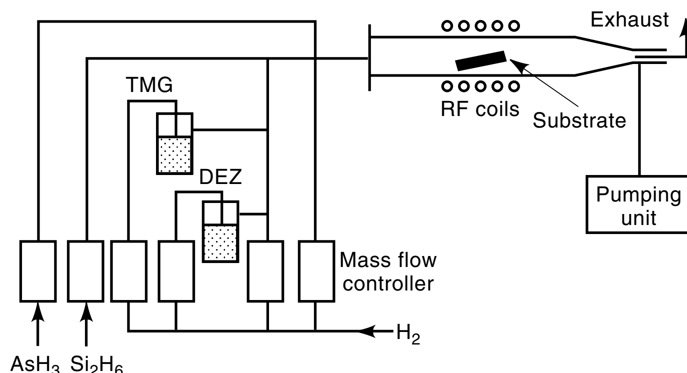

Figure 8. Schematic diagram of a MOCVD system using TMG and AsH_3 sources for the growth of GaAs. Diethylzinc (DEZ) and disilane (Si_2H_6) are *p*- and *n*-type dopant sources, respectively. The metalorganic compounds and hydride sources decompose on the substrate surface situated on an RF inductance heated susceptor.

cold wall reactor by bubbling H_2 through the liquid source, which is held in a temperature-controlled bubbler. Arsenic is transported in the hydride form (i.e., AsH_3). In addition, dopant sources either in hydride forms or metalorganic forms are injected into the reactor to achieve the desired electrical conductivity. Disilane (Si_2H_6) and diethylzinc (DEZ) are the typical *n*- and *p*-type dopants used in the MOCVD growth of III–V compounds, respectively. The substrate is heated on an inductively heated susceptor to a temperature of 600 °C to 800 °C. The metalorganic compound and the hydride diffuse through the boundary layer and decompose on the hot substrate surface in an irreversible reaction to form a GaAs epilayer according to

$$Ga(CH_3)_3 + AsH_3 \rightarrow GaAs + 3CH_4 \qquad (10)$$

or

$$Ga(C_2H_5)_3 + AsH_3 \rightarrow GaAs + 3C_2H_6 \qquad (11)$$

Because the reaction is irreversible and no thermodynamic equilibrium is involved, a very wide range of growth conditions and abrupt compositional changes of epitaxial structures are possible.

Temperature-dependent growth rates have been studied to understand the growth mechanism of MOCVD. Taking GaAs as an example, as seen in Fig. 7, for an AsH_3 to TMG ratio much larger than one, the growth rate is nearly independent of temperature over the range 550 °C to 750 °C (15). This behavior indicates that the growth is determined by diffusion of the TMG species through the boundary layer to the substrate. In this regime, the available metalorganic Ga is the growth-limiting factor, and the growth rate is found to be linearly proportional to the TMG flow rate and independent of arsine partial pressure. In the high-temperature region (≥750 °C), as a result of the desorption of Ga atoms, As molecules, and/or decomposition of the GaAs, the growth rate is under the thermodynamic limitation and begins to decrease. On the other hand, as a result of the inefficient pyrolysis, the growth rate falls off with decreasing temperature below 550 °C.

In growing heterostructures by atmospheric pressure MOCVD, changing the layer composition is carried out by switching flows of metalorganic reactant mixtures. The time required to establish a stable flow with minimum turbulence in the reactor prevents the formation of a sharp interface. The growth of indium-containing compounds from trimethylindium (TMI) or triethylindium (TEI) is further complicated by the possible formation of adducts between hydrides and indium-alkyls. To minimize these problems, low-pressure MOCVD (LP-MOCVD) has been developed (16). LP-MOCVD is usually carried out in a horizontal reactor under reduced pressure in the range of 50 torr to 100 torr. The large reduction of system pressure and increased flow rate enhance the gas-phase transfer of reactants to, and by-products from, the substrate surface. The practical consequences of these results are very significant. Under low-pressure conditions, the high gas flow rate permits rapid establishment of new gas compositions, which lead to more abrupt changes in composition. Furthermore, a more uniform boundary layer thickness is established under high gas flow rates leading to good uniformity in layer thickness and composition. Additionally, the reaction

rate is slowed and reaction time is reduced, which, under low pressure conditions, leads to a minimum adduct formation and a reduced growth rate of about 2 μm/h to 5 μm/h.

For the growth of $A_x^{III}B_{1-x}^{III}C^V$ ternary compounds by MOCVD under a high V/III flow rate ratio, the solid composition x is determined by

$$x = \frac{J_A^{III}}{(J_A^{III} + J_B^{III})} \tag{12}$$

where J is the flux of the group III element. For the growth of alloys with mixing on a group-V sublattice (i.e., $A^{III}C_y^V D_{1-y}^V$), the solid composition y becomes a nonlinear function of vapor composition. This is because of the unequal pyrolysis rates of different group V reactants at the growth temperature. For example, in $GaAs_{1-y}P_y$, a very large ratio of PH_3 to AsH_3 is required to produce alloys with a significant phosphorus content below 750 °C (15).

MOLECULAR BEAM EPITAXY

Pioneered by A. Y. Cho at Bell Laboratories, molecular beam epitaxy is an ultra-high vacuum (UHV) deposition technique with several important features. The MBE growth of semiconductor films takes place by the reaction of molecular beams of the constituent elements with a crystalline substrate surface held at a suitable substrate temperature under UHV conditions. The kinetically controlled MBE growth process involves a series of events: adsorption, surface migration and dissociation, and incorporation. In the case of MBE growth of GaAs, in the absence of free surface Ga adatoms, the impinging As_2 molecules will simply re-evaporate from the surface above 500 °C. Dissociation of adsorbed As_2 and subsequent incorporation into the GaAs lattice can occur only when they encounter paired Ga lattice sites while migrating on the surface. Therefore, for the MBE growth of a stoichiometric GaAs epitaxial layer, it is required that only an excess of As species be present while the growth rate is determined by the arrival rate of the Ga flux.

The unique feature of MBE is the ability to prepare epitaxial layers with atomic dimensional precision down to a few angstroms. This ability allows the preparation of novel devices with multilayered epitaxial structures tailored to meet specific needs. Because MBE is done in a UHV environment, many surface analysis techniques may be used during the growth process. This makes the MBE process a highly controllable and reproducible epitaxy method.

MBE Apparatus

The modern MBE system uses a modular configuration that contains a number of building blocks, such as the growth chamber, the sample exchange load-lock, the surface processing chamber, and the surface analysis chamber, which are all interconnected by a UHV transfer tube. A basic MBE system for III–V compounds is shown in Fig. 9 (17). The UHV growth chamber is evacuated with a pumping stack that maintains a base pressure of 10^{-11} torr. In addition, a liquid-nitrogen-cooled shroud is used to enclose the entire interior surface of the growth chamber in order to minimize contamination from residual water vapor and hydrocarbons during epitaxy. The sample exchange load-lock permits the maintenance of UHV in the growth chamber while changing substrates between successive growth runs.

The substrate is typically mounted on a molybdenum substrate holder attached to a sample manipulator for precise positioning within the growth chamber. The substrate holder can rotate continuously to achieve extremely uniform epitaxial layers. Thermal radiation generated by resistance heating from behind the substrate holder is employed to heat the substrate. On the back side of the manipulator is an ion gauge for beam flux measurements. When rotating the manipulator into position such that the movable ion gauge is facing the effusion cells, the relative flux of each beam can be estimated.

The source flange on the growth chamber contains a viewport and eight or more ports for mounting effusion cells and/or gas injectors. The viewport facilitates the mounting of an optical pyrometer for substrate temperature measurement as well as providing a means of directly viewing the substrate during growth. Ultrahigh purity elemental source materials and dopants loaded in pyrolytic BN effusion cell crucibles are used to generate the desired molecular beams. The effusion cell temperatures are controlled to an accuracy of ± 1 °C to provide the precise amount of beam flux. To initiate or terminate the molecular beam flux, each source is provided with its own externally controlled mechanical shutter. Shutters in front of the orifices can be opened and closed within a tenth of a second, which is much shorter than the typical MBE growth rate of one to two monolayers per second, resulting in abrupt interfaces in the range of one atomic layer. Therefore, the sequence of opening and closing different shutters determines the multilayer heterostructure in terms of both composition and doping profile.

In Situ Surface Diagnosis Techniques

In addition to the components used directly for the MBE growth process, the growth chamber may contain various pieces of in situ surface analysis equipment to monitor the surface structure and control the growth conditions. For a modern MBE system to be used for the production of devices, only a reflection high-energy electron diffraction (RHEED) apparatus and a movable ion gauge in the growth chamber are essential.

The RHEED apparatus provides information concerning substrate cleanliness, smoothness, and surface structure before and during growth as a function of growth conditions. To generate RHEED patterns, as shown in Fig. 9, a collimated beam of high-energy electrons in the range of 5 keV to 40 keV is directed at an angle of 1° to 2° toward the sample surface orthogonal to the molecular beam paths. Because the de Broglie wavelength of an electron at this energy is a fraction of the atomic spacing on the surface, a diffraction pattern is formed on the fluorescent screen mounted opposite the electron source. In this configuration, the sample surface can be continuously monitored without interrupting the growth procedure. On an atomically flat surface, it shows a streaked RHEED pattern normal to the shadow edge of the sample. Otherwise, the diffraction pattern from a rough surface is formed mainly in transmission through the surface asperities and exhibits a spotty appearance. Figure 10 is an example of the (100) GaAs surface morphology evolution during the initial stages of the MBE growth and their corresponding

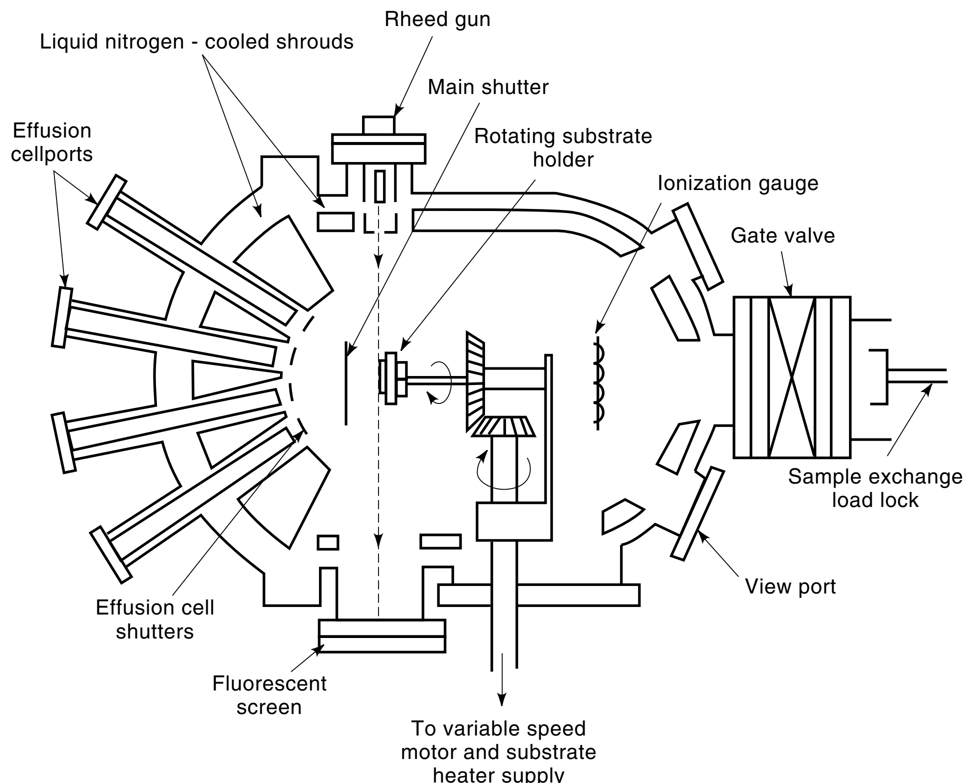

Figure 9. Cutaway view of a modern molecular beam epitaxy system viewed from the top. Molecular beams are generated from effusion cells and/or gas injectors mounted on the source flange. Opening and closing of different shutters in front of effusion cell orifices determines the heterostructure grown on the heated substrate. (Reprinted with permission from A. Y. Cho and K. Y. Cheng, Growth of extremely uniform layers by rotating substrate holder with molecular beam epitaxy for applications to electro-optic and microwave devices, *Appl. Phys. Lett.,* **38**: 360–362, 1981. © 1981 American Institute of Physics.)

RHEED patterns (18). The clean but rough starting surface shows a spotty bulk RHEED pattern as seen in Fig. 10(a). The RHEED pattern changes from spotty to streaky as the surface is smoothed out.

In addition to the spotty-to-streaky transition in the RHEED patterns of a clean crystal surface during growth, additional light streaks appear half-way between the elongated bulk spots along the $[\bar{1}\bar{1}0]$ azimuth as seen in Figs. 10(b) and (c). These added features represent the rearrangement of atoms on the surface in order to accommodate the surface dangling bonds and to minimize the surface free energy. Depending on the surface-atom coverage conditions and the electron beam incident directions, the pattern of extra diffraction lines between the bulk streaks assumes different forms. The RHEED patterns of Ga-rich (Ga-stabilized) surfaces and As-rich (As-stabilized) surfaces are similar except interchanged along $[\bar{1}10]$ and $[1\bar{1}0]$ azimuthes. In real space, the two surface structures are related by a simple rotation of 90° about the [001] direction. The relationships between the surface structures and the growth conditions (i.e., the surface phase diagram) of (100) GaAs have been established in terms of As_4/Ga flux ratios and substrate temperatures (19). From the point of view of practical GaAs growth, the As-stabilized structure is preferred. A high-quality smooth (100) GaAs surface can be achieved under this condition. On the other hand, prolonged growth under Ga-stabilized condition leads to a dull surface caused by the formation of Ga droplets. Overall, because of its simplicity and in situ nature, the RHEED technique is routinely used in MBE to monitor the surface cleaning process prior to epitaxial growth and to optimize growth conditions during growth.

Flux Control of Molecular Beams

For an ideal Knudson-type effusion cell, the beam flux arriving at the substrate surface positioned at a distance d (cm) from the aperture can be calculated as follows:

$$J = 1.118 \times 10^{22} \frac{pA}{d^2\sqrt{MT}} \cos\theta \qquad (\text{molecules-cm}^{-2}\text{-s}^{-1}) \quad (13)$$

where p (torr) is the pressure in the cell, A (cm^2) is the area of the aperture, M is the molecular weight, T (K) is the temperature of the cell, and θ is the angle between the beam and the normal of the surface. However, this equation serves only as a guideline because, in practice, the ideal pinhole-size cell aperture is enlarged to enhance the growth rate. The beam fluxes emerging from these nonideal effusion cells are generally determined experimentally.

For in situ calibration of beam fluxes and growth rates, the most convenient and routinely used method is the RHEED intensity oscillation technique (20). As shown in Fig. 11, the equilibrium surface existing before growth is smooth, corresponding to high reflectivity of the specular beam. As growth commences, nucleation islands will form at random sites on the surface, leading to a decrease in reflectivity. These islands grow in size until they coalesce into a smooth surface again. It is expected that the minimum in reflectivity would correspond to 50% coverage by the growing layer. Therefore, the period of the oscillations corresponds precisely to the growth rate of a monolayer. Because the sticking coefficients of the group III elements are unity, once the beam fluxes and the growth rates are calibrated, the alloy composition in the A^{III}–B^{III}–C^{V} alloy is simply determined by the relative group

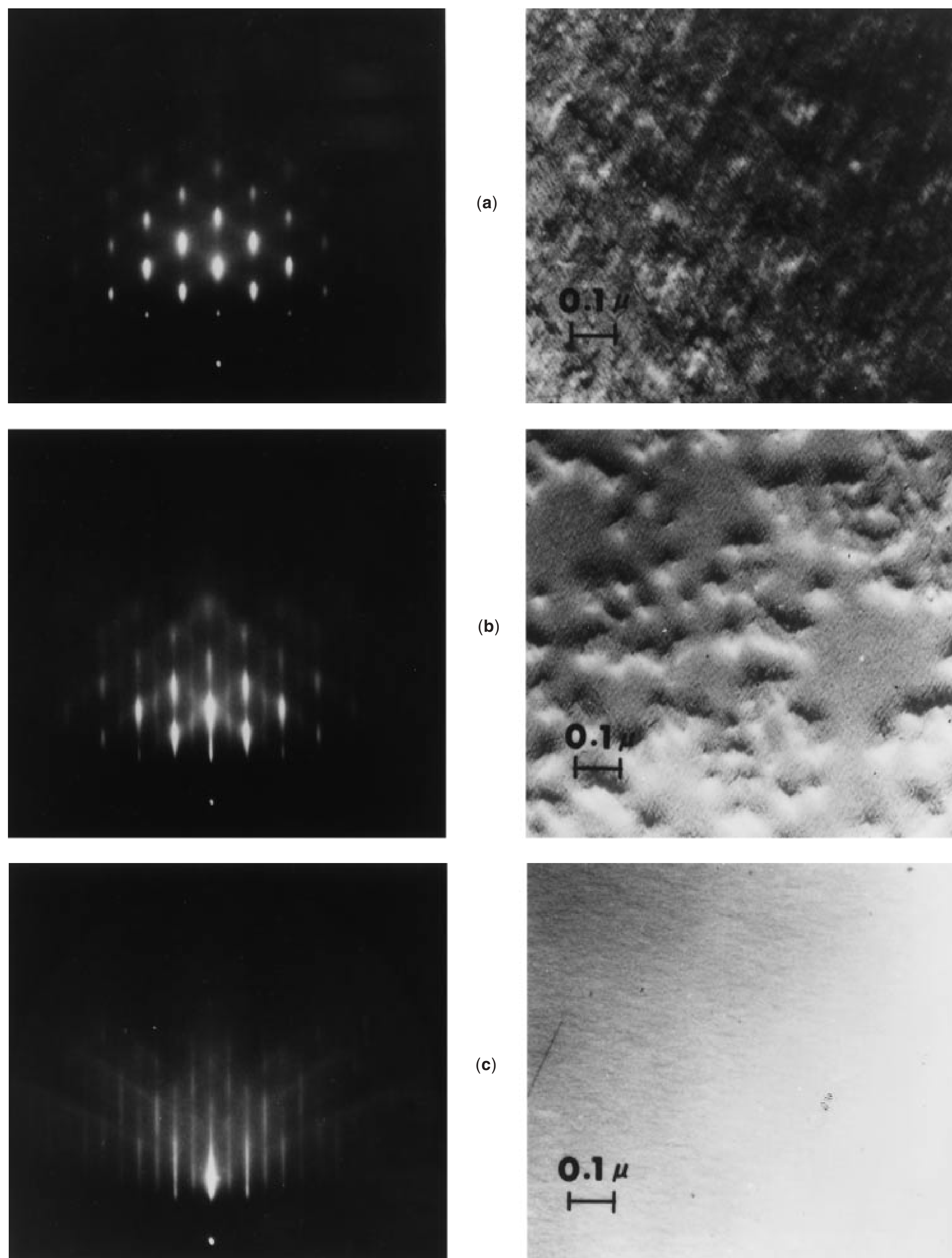

Figure 10. 40 keV RHEED patterns of a (100) GaAs surface taken at $[\overline{1}\overline{1}0]$ azimuth and the corresponding photomicrographs; (a) after chemical etching and heating to 580 °C, (b) after depositing 150 Å of GaAs, and (c) after depositing 1 μm of GaAs. (Reprinted with permission from A. Y. Cho, Film deposition by molecular beam epitaxy, *J. Vac. Sci. and Technol.,* **8**: S31–38, 1971. © 1971 American Institute of Physics.)

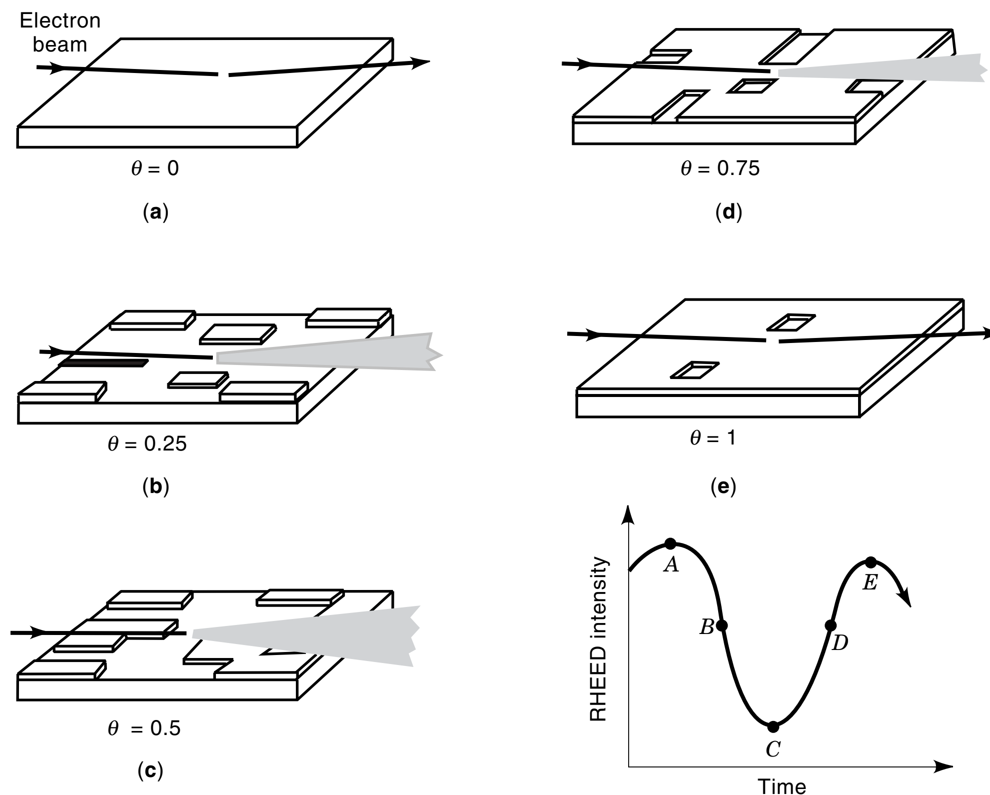

Figure 11. Real space representation of the formation of the first complete monolayer of (001) GaAs with respect to RHEED intensity oscillations. The intensity of the diffracted electron beam decreases as surface roughness increases. θ is the fractional layer coverage. The period of the oscillation, for example, time span between point A and point E, corresponds to the growth rate of one atomic layer.

III fluxes reaching the surface. For example, the Al fraction in $Al_xGa_{1-x}As$ can be determined by the relation

$$x = \frac{R(Al_xGa_{1-x}As) - R(GaAs)}{R(Al_xGa_{1-x}As)} \tag{14}$$

where R is the growth rate.

Variation of Molecular Beam Sources

Although MBE has been successful for the growth of arsenic and antimony compounds, the growth of phosphorus compounds by conventional solid source MBE (SSMBE) had been hampered by the high vapor pressure and the allotropic property of solid phosphorus. Recently, a new approach for the growth of P-compounds by SSMBE has also been developed (21). This technique uses a three-zone valved cracking cell to generate P_2 molecules. The structure of solid-P valved cracking cell consists of a red P oven, a white P condensing reservoir, and a valved thermal cracking region. During operation, the red P oven is heated to an appropriate temperature in order to generate a sufficient amount of P_4 vapor. The white P reservoir section during this time period is held at a low temperature to condense the vapor into white P while the valve is closed. After the desired quantity of white P has been collected, both the red P oven and the white P reservoir are returned to ambient temperature to finish the distillation process. The P_4 vapor emanating from the white P reservoir is passed through the high-temperature cracking zone and dissociated into P_2 at the desired rate via the adjustable flux control valve. The accumulated white P and its associated high vapor pressure enable the condensing reservoir to be operated at room temperature during growth. This capability strongly inhibits the formation of multiple allotropes and makes accurate P flux control possible. Highly reproducible growth of P-compounds and device structures have been demonstrated.

The gas source molecular beam epitaxy (GSMBE) technique, in which the elemental As and P sources are replaced by gaseous AsH_3 and PH_3, respectively, represents an alternative approach (22). Further development of the technology is to replace the group III elements with gas sources. This is conveniently accomplished using metalorganic group III species in addition to hydride group V sources. This method is generally referred to as metalorganic molecular beam epitaxy (MOMBE) or chemical beam epitaxy (CBE). Both GSMBE and MOMBE use the same growth system design similar to SSMBE with modifications in source delivery and UHV pumping methods.

GSMBE and MOMBE use gas-handling systems similar to those used by MOCVD to deliver gas sources into the UHV growth chamber for epitaxy. The major distinction between the GSMBE/MOMBE method and MOCVD centers around the pressure regimes involved in each method. Namely, the latter operate under viscous flow and the former, under mo-

lecular flow conditions. In molecular flow, the pressure inside the growth chamber is low ($<10^{-4}$ torr), and there exists no effective boundary layer at the growing interface. This leads to a GSMBE/MOMBE beam flux control very similar to SSMBE, and all the analytical equipment ordinarily used to monitor the process can be implemented in the same way.

In GSMBE, after the hydrides have been delivered into the growth chamber, they are thermally cracked at high temperatures. To improve the quality of grown layers and for safety reasons, the hydride gas injector should be able to generate a significant enhanced dimer to tetramer ratio (V_2/V_4) and an improved cracking efficiency (≥99.9%) for both AsH_3 and PH_3 with a minimum switching transient. In the case of MOMBE, the group III metalorganic species, similar to those used in MOCVD, are also delivered from a gas source into the UHV growth chamber through a single gas injector. Unlike the group V hydrides, the mixed group III metalorganics are not predecomposed, and pyrolysis occurs only on the heated substrate surface to prevent any chemical reactions in gas phase. Therefore, the chemical reactions at the growing surface in MOMBE are expected to be considerably more complex than in the case of GSMBE. On the other hand, the lack of a boundary layer on the growth surface in MOMBE makes the surface reaction chemistry different from that in the case of MOCVD.

Gallium nitride and related compounds have recently emerged as the leading material for fabricating blue-green light emitters and high temperature electronic devices. For the MBE growth of III–V nitride compounds using nitrogen gas source, the stable chemical bonds of molecular nitrogen in a low background pressure environment makes thermal cracking unsuccessful in generating abundant atomic nitrogen for epitaxial growth. To supply sufficient energy in breaking chemical bonds of molecular nitrogen, the electron-cyclotron resonance (ECR) microwave plasma source and RF plasma source techniques have been developed (23). In these approaches, the microwave or RF energy is coupled into the nitrogen plasma to crack molecular nitrogen efficiently into atomic sources of nitrogen suitable for III–V nitride compound growth.

SELECTIVE EPITAXY

Over the years, epitaxial growth techniques have advanced significantly with the demonstration of excellent control in composition, doping profile, and thickness along the growth direction. In order to form three-dimensional structures for novel or more functional devices, there has been a need to attain growth control in the lateral direction as well. To form such three-dimensional structures, the most common approach is to use selective area growth over patterned substrates.

Using a thin dielectric film deposited on the substrate as the mask, one can selectively grow active devices in open window areas formed by lithographic techniques. Because the LPE process is carried out under near-equilibrium condition, the epitaxial growth will occur only in the window area, and no nucleation will be formed on the oxide-covered mask area. Selective area epitaxy by MOCVD over masked surfaces ends up with a similar result but for a different reason. Metalorganic source material arriving from the gas phase will grow

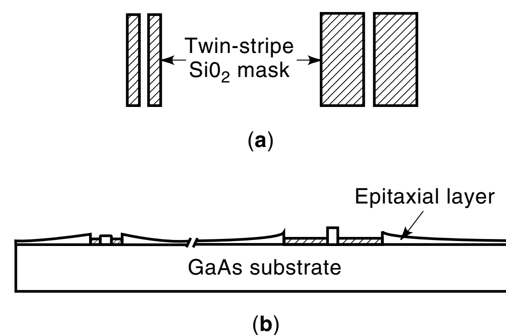

Figure 12. Schematic of (a) the SiO_2 mask and (b) the relative thickness variation in unmasked areas on a twin-stripe mask GaAs structure. The enhancement of growth rate in between the twin-stripe SiO_2 mask increases with the mask width.

epitaxially in regions where there is no mask. Because of a very low adsorption, the source material that lands on the dielectric mask will travel a finite distance before returning to the gas phase, resulting in no growth. If the source material arrives at the mask edge, it will nucleate on the semiconductor surface and enhance the thickness around the edge. For the case of a twin-stripe masked substrate with a narrow center opening, one can use this method to modify the growth rate and composition in the center window area by selecting different mask stripe widths. As shown Fig. 12, this technique allows the engineer to determine selectively the local bandgap of many different devices within a single plane simultaneously using different mask strip widths. However, in MBE the near-unity sticking coefficient of the elemental group III sources results in the growth rate in the window area and on the mask to be the same such that selective area epitaxy will not occur. Consequently, a single crystal will grow in the window area, and high-resistivity polycrystalline materials will grow on the dielectric-covered area, resulting in planar growth of isolated devices. In contrast, similar to MOCVD where growth relies on the catalyzed surface decomposition of metalorganics, MOMBE will only grow in the window area, and no nucleation will occur on the dielectric-covered area resulting in nonplanar selective growth.

The other form of selective epitaxy is to carry out regrowth on a pre-etched, nonplanar (channeled) substrate. In this case, LPE and VPE will fill the channels resulting in a planar structure, whereas MBE will preserve the channeled substrate geometry of nonplanar growth. In LPE, from thermodynamic considerations, variations in surface curvature are associated with variations in chemical potential of the solid (24).

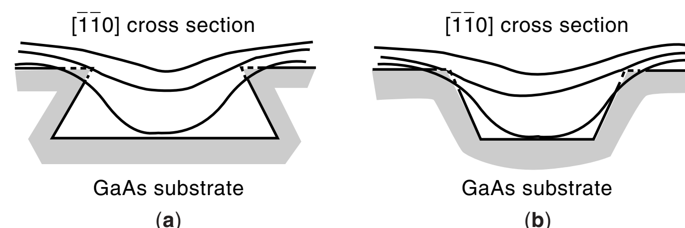

Figure 13. Schematic representation of liquid-phase epitaxial growth stages over channeled GaAs substrates along (a) $[\bar{1}\bar{1}0]$ and (b) $[\bar{1}10]$ directions. The dotted lines indicate the original channel profiles.

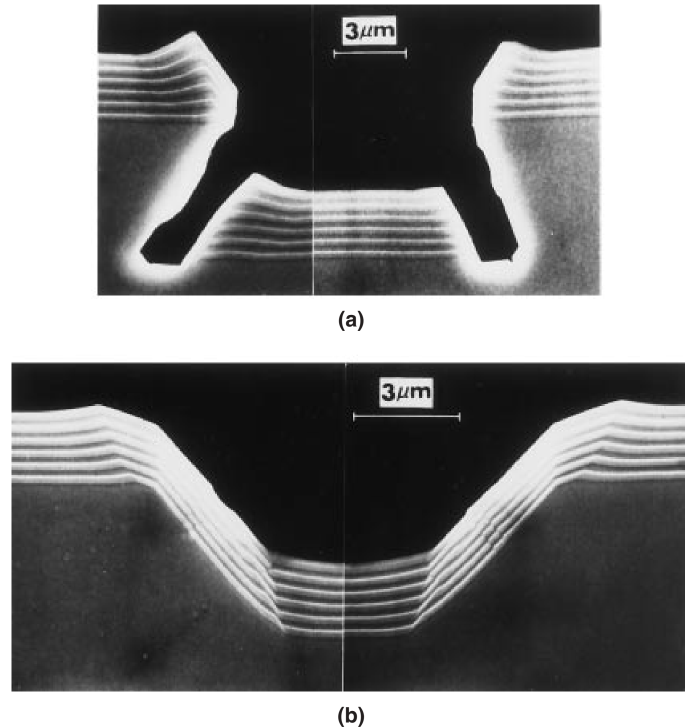

Figure 14. Cross-sectional scanning-electron microscope photos of alternating GaAs and $\underline{Al}_{0.2}Ga_{0.8}As$ multilayer structures over channels aligned along the (a) $[\bar{1}\bar{1}0]$ and (b) $[1\bar{1}0]$ directions. (Reprinted with permission from W. T. Tsang and A. Y. Cho, Growth of GaAs—$Ga_{1-x}Al_xAs$ over preferentially etched channels by molecular beam epitaxy, *Appl. Phys. Lett.,* **30**: 293–296, 1977. © 1977 American Institute of Physics.)

In order to maintain equilibrium at the solid-liquid interface, the variations in chemical potential of the solid must be matched by variations in the local solute concentration. As shown in Fig. 13, the net result is that the melt tends to fill in concave parts of the surface and melt-back convex parts of the surface. The local solute concentration gradients between melt-etched areas and filled areas will further enhance this lateral mass transfer. For VPE growth, the kinetic process limits the surface reaction rate and leads to a growth rate dependent on crystallographic orientation (13). However, the prediction of growth rates under different growth conditions is complicated by the lack of detailed understanding of surface and gas-phase reactions In general, low growth rates are observed on most low index faces (100), (110), and (111)B, but the maximum rate is observed near (111)A. In practice, the etching conditions used to expose different micro facets in etched channels, coupled with a properly adjusted growth temperature and reactant flow rates, result in the desired morphology for opto-electronic device fabrication. On the contrary, as a result of the uniform and unidirectional beam flux properties, the MBE growth morphology over a patterned surface is primarily determined by the surface migration length of the adatoms and the anisotropy of growth rates on various crystal planes. As shown in Fig. 14, for an open channel structure (e.g., flat-bottom V-groove), it will preserve the geometry of the channel surface (25). On the other hand, because of the beam nature associated with the molecular fluxes, the overhanging edges of dove-tail shaped channels may be used as self-aligned masks to grow isolated ridges within channels.

UNIQUE DEVICE STRUCTURES

Modulation-Doped Field-Effect Transistors

Using modern epitaxy techniques, many new device structures are designed and artificially fabricated to give new electronic and photonic properties that do not exist in bulk materials. One such example is the modulation-doped field-effect transistor (MODFET) also known as high electron mobility transistor (HEMT) (26). This device has been widely used in low-noise microwave receivers of systems like direct broadcasting satellite TVs. The working principle of the MODFET is based on modulation doping or selective doping in heterostructures such that mobile electrons are separated from their parent impurity donors. This is in contrast to the conventional FET where electrons travel through the doped part (conduction channel) of the crystal. Ionized impurity-induced electrostatic interaction disturbs the electron motion and results in less ideal transport properties.

Figure 15 shows the heterostructure and the energy-band diagram of a GaAs—$Al_xGa_{1-x}As$ MODFET where impurities are introduced into the large bandgap $Al_xGa_{1-x}As$ selectively. At equilibrium, electrons from donors in $Al_xGa_{1-x}As$ move to the undoped GaAs conduction channel leaving behind ionized donors. These electrons are further confined by electrostatic forces within ~10 nm of the GaAs—$Al_xGa_{1-x}As$ interface and

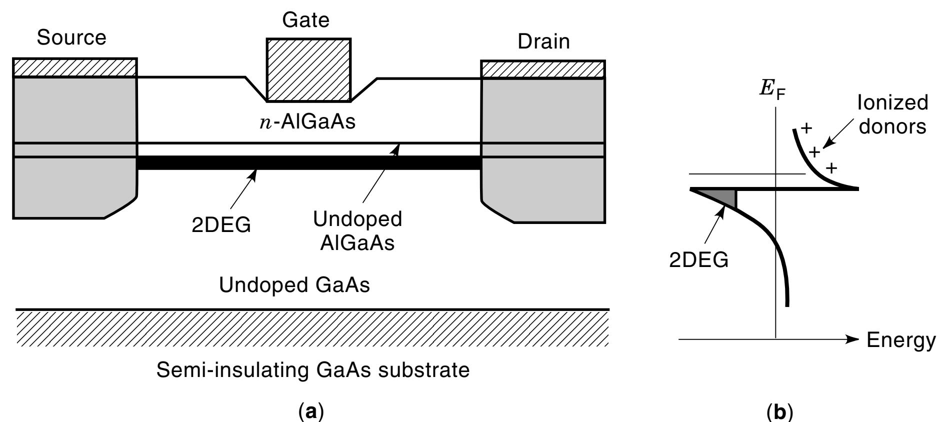

Figure 15. (a) The device structure and (b) the band-edge diagram of a typical $Al_xGa_{1-x}As$ modulation-doped field-effect transistor. The majority of the $Al_xGa_{1-x}As$ layer is doped with Si impurity atoms except close to the $Al_xGa_{1-x}As$–GaAs heterojunction and the GaAs layer is not intentionally doped. Electrons originating from the Si-doped $Al_xGa_{1-x}As$ layer transfer to the GaAs layer forming a 2DEG in the quantum well at the heterojunction interface. Due to the lack of scattering with impurities within the 2DEG conduction channel, electrons can move between source and drain with great velocity resulting in high operation speed.

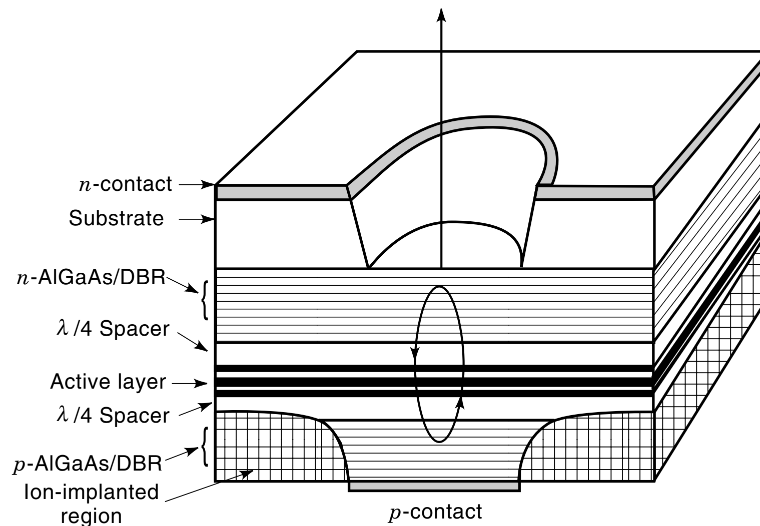

Figure 16. Schematic of a vertical-cavity surface-emitting laser with epitaxially grown superlattice distributed Bragg reflection mirrors. For efficient operation, a proton implant region is placed immediately adjacent to the optical cavity to produce a current blocking layer, funneling current through a small region of the active layer. The light emission direction can take place in either the epilayer side or the substrate side. In this device, the bottom emitting structure is used where the laser light is emitted through an etched hole in the substrate.

form a two-dimensional electron gas (2DEG). The lack of scattering with impurities within the 2DEG enhances the electron mobility, resulting in high operation speeds. In 1989, the electron mobility of modulation doped GaAs structures at low temperatures had reached 10^7 $cm^2/V \cdot s$, which is over three orders of magnitude higher than the bulk crystal. Nevertheless, the success of MODFETs depends heavily on the GaAs—$Al_xGa_{1-x}As$ interface quality. Because the 2DEG is confined at the interface, any interface roughness will degrade the electron transport properties. In addition, the MODFET performance also depends on the doping and thickness control in the $Al_xGa_{1-x}As$ layer. Any variations in these two parameters will prevent a consistent performance. The highly precise and reproducible properties have made MBE technique an ideal method to prepare MODFET structures.

Vertical-Cavity Surface-Emitting Lasers

Semiconductor lasers emitting light from normal to the substrate surface are emerging as a promising solution for fabricating low-cost and high-performance lasers for applications in optical communication, optical interconnects, and optical signal processing. The vertical-cavity surface-emitting laser (VCSEL) uses a pair of highly reflective mirrors cladding the active region to form a vertical laser resonance cavity that produces a laser beam normal to the substrate surface (27). It offers several advantages over the conventional edge-emitting lasers including on-wafer preprocess screening of laser samples, single-frequency and low-divergence circular beam, and easy integration into 2-D arrays. Figure 16 shows the structure of a typical $Al_xGa_{1-x}As$ VCSEL. A pair of GaAs/$Al_xGa_{1-x}As$ distributed Bragg reflectors (DBR) consisting of periodic quarter-wavelength stacks of low and high refractive index $Al_xGa_{1-x}As$ and GaAs are used for reflecting mirrors of the laser. The reflectivities of these DBR mirrors are critical to the successful operation of the laser. To achieve very high reflectivities (>99%) in these DBRs, near 100 quarter-wavelength mirror layers are needed. Furthermore, in order to place the Fabry–Pérot resonance at the exact wavelength for lasing, the thickness and alloy composition of all these layers has to be precisely controlled to less than 1% variation. These requirements make the growth task rather demanding. Although the surface-emitting lasers have been explored since the 1970s, the GaAs-based VCSEL was successfully demonstrated only after highly precise growth techniques such as MOCVD and MBE methods became mature in the early 1990s.

BIBLIOGRAPHY

1. For a review, see, e.g., J. J. Hsieh, Liquid phase epitaxy. In T. S. Moss (ed.), *Handbook of Semiconductors,* vol. 3, New York: North-Holland, 1980, pp. 415–497.
2. For a review, see, e.g., G. Beuchet, Halide and chloride transport vapor-phase deposition of InGaAsP and GaAs. In W. T. Tsang (ed.), *Semiconductors and Semimentals,* vol. 22, part A, Orlando, FL: Academic Press, 1985, pp. 261–297.
3. For a review, see, e.g., A. Y. Cho, *Molecular Beam Epitaxy,* New York: American Institute of Physics, 1994.
4. For a review, see, e.g., G. B. Stringfellow, *Organometallic Vapor-Phase Epitaxy: Theory and Practice,* Boston: Academic Press, 1989.
5. H. Nelson, Epitaxial growth from the liquid state and its application to the fabrication of tunnel and laser diodes, *RCA Rev.,* **24**: 603–615, 1963.
6. M. B. Panish and M. Ilegems, Phase equilibria in ternary III-V systems. In H. Reiss and J. O. McCaldin (eds.), *Prog. in Solid State Chem.,* vol. 7, New York: Pergamon Press, 1972, pp. 39–83.
7. M. Ilegems and M. B. Panish, Phase equilibria in III-V quaternary systems—Application to Al–Ga–In–P, *J. Phys. Chem. Solids,* **35**: 409–420, 1974.
8. A. S. Jordan and M. Ilegems, Solid-liquid equilibria for quaternary solid solutions involving compound semiconductors in the regular solution approximation, *J. Phys. Chem. Solids,* **36**: 329–342, 1975.
9. K. Nakajima, Liquid phase epitaxy. In T. P. Pearsall (ed.), *GaInAsP Alloy Semiconductors,* New York: Wiley, 1982, pp. 43–60.
10. J. J. Hsieh, Thickness and surface morphology of GaAs LPE layers grown by supercooling, step-cooling, equilibrium-cooling, and two-phase solution techniques, *J. Cryst. Growth,* **27**: 49–61, 1974.
11. D. W. Shaw, Chemical vapor deposition. In J. W. Matthews (ed.), *Epitaxial Growth,* part A, New York: Academic Press, 1975, pp. 89–107.

12. G. H. Olsen, Vapor phase epitaxy of GaInAsP. In T. P. Pearsall (ed.), *GaInAsP Alloy Semiconductors,* New York: Wiley, 1982, pp. 11–41.
13. D. W. Shaw, Influence of substrate temperature on GaAs epitaxial deposition rates, *J. Electrochem. Soc.,* **115**: 405–408, 1968.
14. H. M. Manasevit and W. I. Simpson, The use of metal-organics in preparation of semiconductor materials: I. Epitaxial gallium-V compounds, *J. Electrochem. Soc.,* **116**: 1725–1732, 1969.
15. G. B. Stringfellow, Organometallic vapor-phase epitaxial growth of III-V semiconductors. In W. T. Tsang (ed.), *Semiconductors and Semimetals,* vol. 22, part A, Orlando, FL: Academic Press, 1985, pp. 209–259.
16. J. P. Hirtz et al., $Ga_{0.47}In_{0.53}As$/InP and GaInAsP/InP double heterostructures grown by low-pressure Metal-organic vapour-phase epitaxy. In T. P. Pearsall (ed.), *GaInAsP Alloy Semiconductors,* New York: Wiley, 1982, pp. 61–86.
17. A. Y. Cho and K. Y. Cheng, Growth of extremely uniform layers by rotating substrate holder with molecular beam epitaxy for applications to electro-optic and microwave devices, *Appl. Phys. Lett.,* **38**: 360–362, 1981.
18. A. Y. Cho, Film deposition by molecular beam epitaxy, *J. Vac. Sci. Technol.,* **8**: S31–S38, 1971.
19. A. Y. Cho, Growth of III-V semiconductors by molecular beam epitaxy and their properties, *Thin Solid Films,* **100**: 291–317, 1983.
20. J. J. Harris, B. A. Joyce, and P. J. Dobson, Oscillations in the surface structure of Sn-doped GaAs during growth by MBE, *Surf. Sci.,* **103**: L90–96, 1981.
21. J. N. Baillargeon and A. Y. Cho, Molecular beam epitaxial growth of $Ga_xIn_{1-x}P$–GaAs ($x \sim 0.5$) double heterojunction laser diodes using solid phosphorus and arsenic valved cracking cells, *J. Vac. Sci. Technol.,* **B13**: 736–738, 1995.
22. M. B. Panish and H. Temkin, *Gas Source Molecular Beam Epitaxy,* Berlin: Springer-Verlag, 1993.
23. T. Lei et al., Epitaxial growth of zinc blende and wurtzitic gallium nitride thin films on (001) silicon, *Appl. Phys. Lett.,* **59**: 644–646, 1991; S. Guha et al., Surface lifetimes of Ga and growth behavior on GaN (0001) surfaces during molecular beam epitaxy, *Appl. Phys. Lett.,* **69**: 2879–2881, 1996.
24. D. Botez, Liquid-phase epitaxy over channeled substrates, *J. Cryst. Growth,* **70**: 150–154, 1984.
25. W. T. Tsang and A. Y. Cho, Growth of GaAs—$Ga_{1-x}Al_xAs$ over preferentially etched channels by molecular beam epitaxy: A technique for two-dimensional thin film definition, *Appl. Phys. Lett.,* **30**: 293–296, 1977.
26. H. Daembkes (ed.), *Modulation-Doped Field-Effect Transistors: Principles/Design/and Technology,* New York: IEEE Press, 1991.
27. C. J. Chang-Hasnain, Vertical-cavity surface emitting lasers. In G. P. Agrawal (ed.), *Semiconductor Laser: Past, Present, and Future,* New York: Am. Inst. of Phys., 1995, pp. 145–180.

K. Y. CHENG
University of Illinois

EPITAXIAL LAYER SEMICONDUCTORS. See SEMICONDUCTOR EPITAXIAL LAYERS.